Supporting Information for:

PLASTIC MORPHOLOGICAL RESPONSE TO SPECTRAL SHIFTS DURING INORGANIC PHOTOTROPIC GROWTH

KATHRYN R. HAMANN[†], MADELINE C. MEIER[†], NATHAN S. LEWIS[†,‡,*], AZHAR I. CARIM[†,‡,*]

[†]Division of Chemistry and Chemical Engineering
California Institute of Technology
Pasadena, CA 91125

[‡]Beckman Institute
California Institute of Technology
Pasadena, CA 91125

*Corresponding Authors: nslewis@caltech.edu, aic@caltech.edu

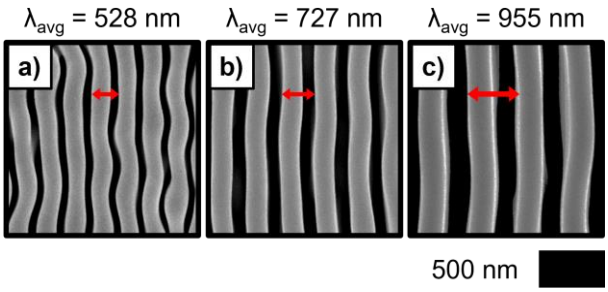

Figure S1. Representative top-view SEMs of films generated using the indicated λ_{avg} illumination for t = 2.00 min with a characteristic feature pitch marked using a double arrow.

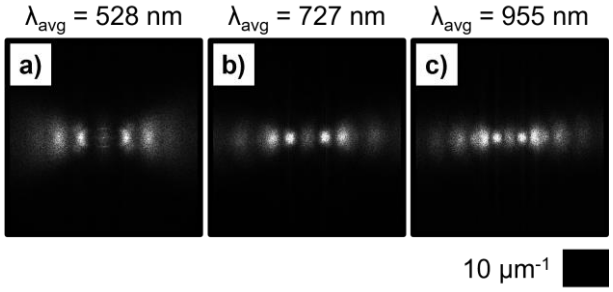

Figure S2. 2D FTs generated from top-view SEM data of films generated using the indicated λ_{avg} for t = 2.00 min.

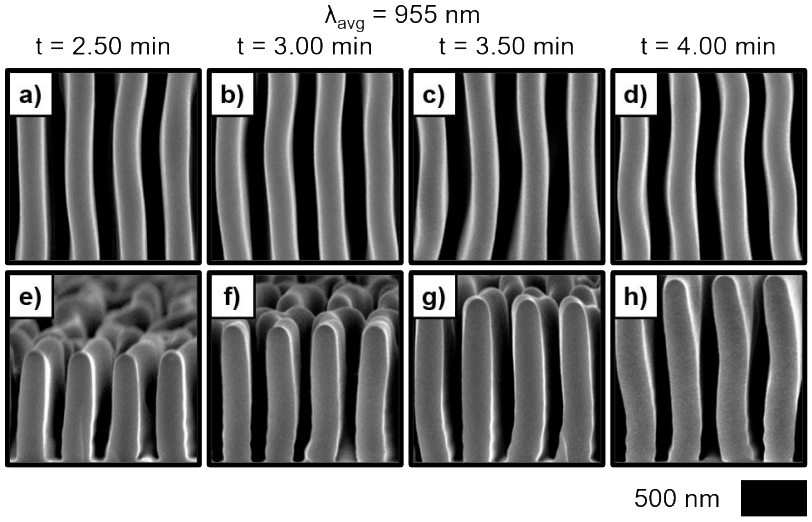

Figure S3. (a)-(d) Representative top-view and (e)-(h) cross-sectional SEMs of films generated using λ_{avg} = 955 nm for the indicated t.

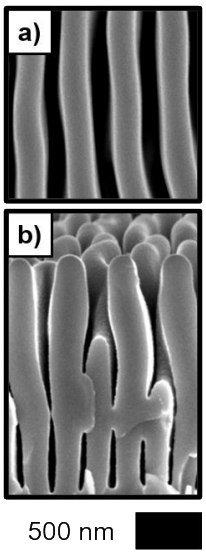

Figure S4. (a) Representative top-view and (b) cross-sectional SEMs of films generated using λ_0 = 727 nm for t_0 = 2.00 min and then extended using λ_1 = 955 nm for t_1 = 3.50 min.

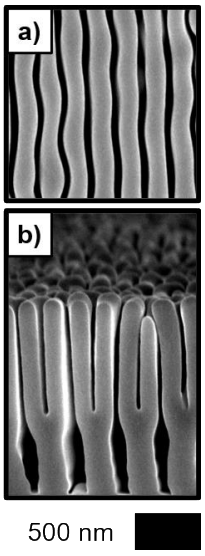

Figure S5. (a) Representative top-view and (b) cross-sectional SEMs of films generated using λ_0 = 955 nm for t_0 = 2.00 min and then extended using λ_1 = 528 nm for t_1 = 3.00 min.

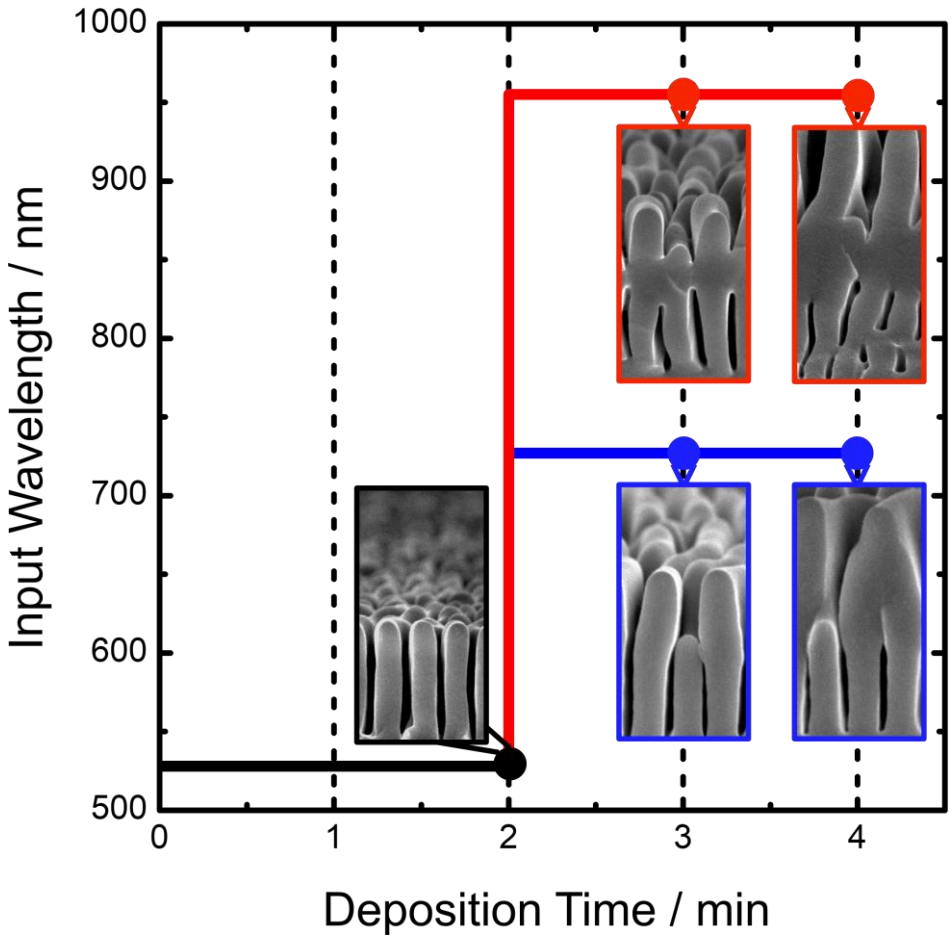

Figure S6. Flowchart with representative cross-sectional SEMs detailing the morphological evolution of films generated initially using λ_0 = 528 nm for t_0 = 2.00 min and then extended in a second deposition step using either λ_1 = 727 nm or 955 nm for the indicated additional time.

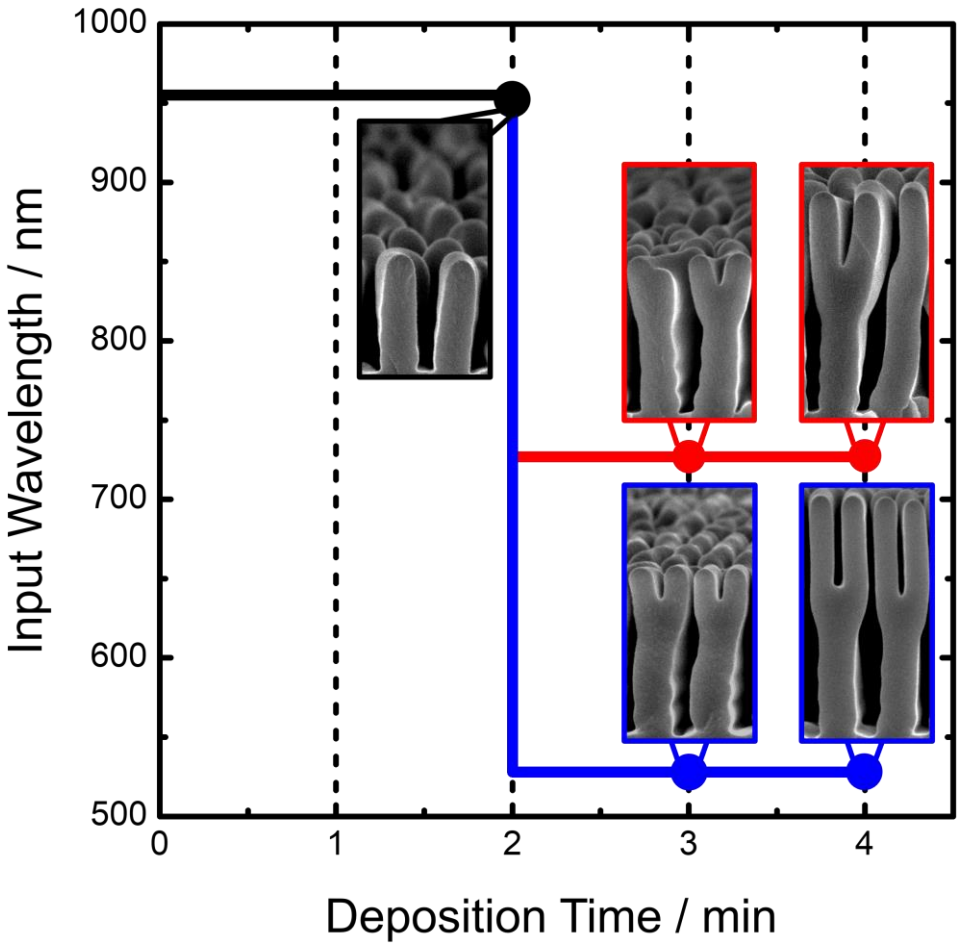

Figure S7. Flowchart with representative cross-sectional SEMs detailing the morphological evolution of films generated initially using λ_0 = 955 nm for t_0 = 2.00 min and then extended in a second deposition step using either λ_1 = 727 nm or 528 nm for the indicated additional time.

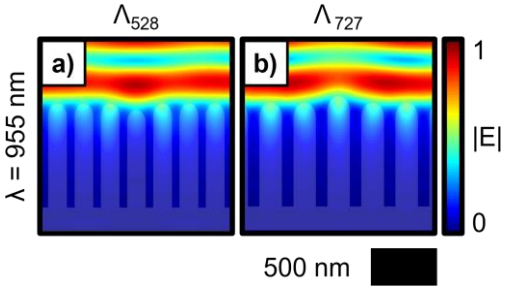

Figure S8. Simulated spatial profiles representing the normalized time-averaged E-field magnitude, |E|, resulting from λ = 955 nm illumination of simplified structures representative of the indicated experimentally observed structures, but with the height of a single feature adjusted to model initial extension using λ_1. Red represents maximal magnitude and blue minimal.

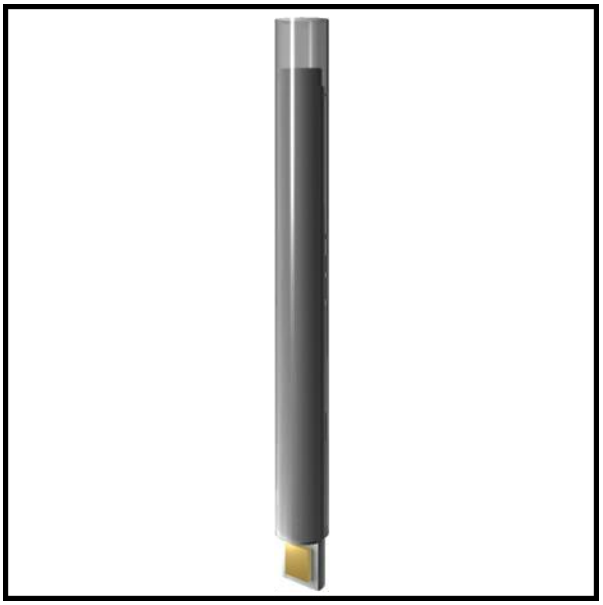

Figure S9. Schematic of an electrode assembly with an attached Au-topped Si section.

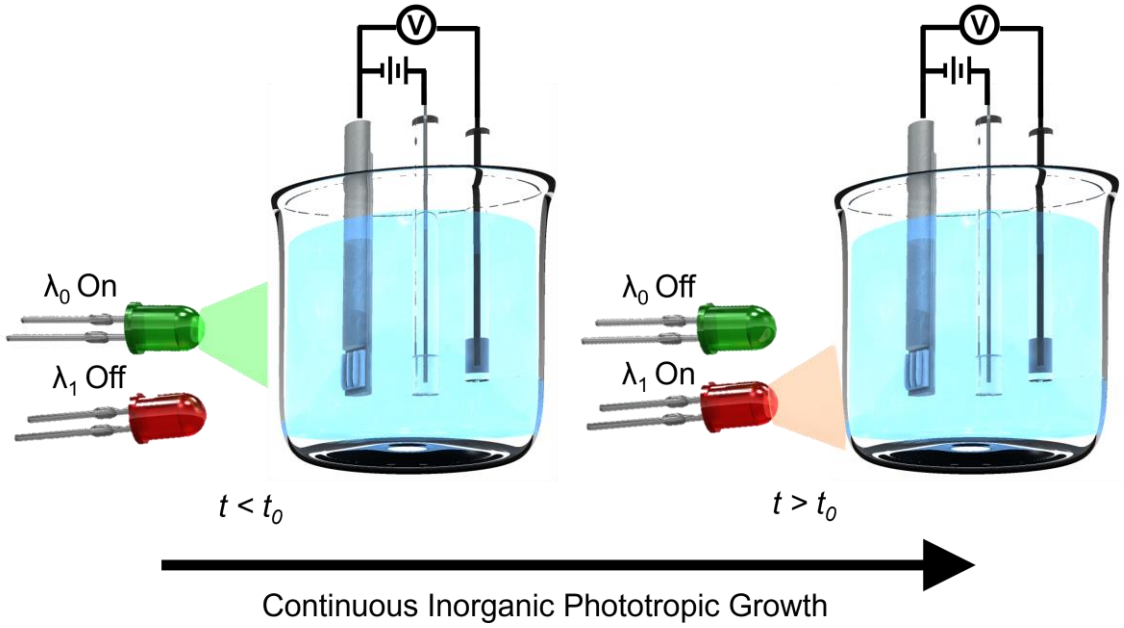

Figure S10. Schematic depicting inorganic phototropic growth using sequential, discrete spectral inputs. For $t < t_0$ (t_0 = 2.00 min), the deposition substrate is illuminated using light from a LED source with an intensity-weighted average emission wavelength of λ_0. Then, at t_0, the LED emitting at λ_0 is turned off, the illumination is replaced with light from a LED source emitting at λ_1, and inorganic phototropic growth is continued with this condition for $t > t_0$.

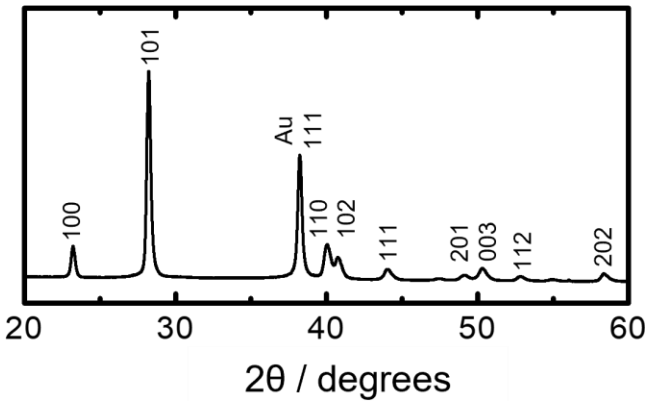

Figure S11. Representative X-ray diffractogram of a Se-Te film with reflections characteristic of Se-Te and the Au substrate indicated.[1,2]

Figure S11 presents a representative X-ray diffractogram of a Se-Te film. The reflections in this diffractogram are consistent with a substitutional alloy of Se and Te in a trigonal crystal structure common to each element in the pure phase and indicate a polycrystalline film.[1,2]

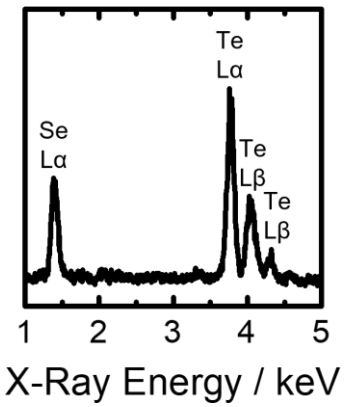

Figure S12. Representative energy-dispersive X-ray spectrum of a Se-Te film.

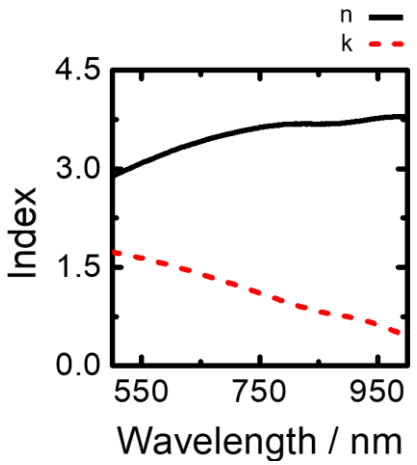

Figure S13. Complex refractive index of characteristic of a Se-Te film.

The wavelength-dependent complex index of refraction values characteristic of Se-Te were derived from experimentally acquired spectroscopic ellipsometry data. A J. A. Woollam VASE ellipsometer was used to obtain amplitude ratio and phase difference (Ψ and Δ) data from electrodeposited Se-Te material, and the WVASE software package (J. A. Woollam) was utilized to calculate from this data the complex index of refraction which is presented in Figure S13.

λ_{avg} / nm	n	k
528	3.00	1.68
727	3.59	1.18
955	3.77	0.62

Table S1. Point values of the real and imaginary parts of the complex refractive index characteristic of deposited Se-Te at the λ_{avg} values utilized in this work.

Average Wavelength Weighted by Intensity / nm	Average Wavelength Weighted by Photon Count / nm
528	529
727	727
955	956

Table S2. Average emission wavelengths of the LED sources used in this work as weighted by intensity (λ_{avg}) and by photon count.

REFERENCES

(1) Smith, T. W.; Smith, S. D.; Badesha, S. S. Chemical Alloying, a Novel Method for the Preparation of Homogenous Se_xTe_{1-x} Alloys. *J. Am. Chem. Soc.* **1984**, *106*, 7247-7248.

(2) Mayers, B.; Gates, B.; Yin, Y.; Xia, Y. Large-Scale Synthesis of Monodisperse Nanorods of Se/Te Alloys Through a Homogenous Nucleation and Solution Growth Process. *Adv. Mater.* **2001**, *13*, 1380-1384.